A Neuronal Model for Visually Evoked Startle Responses in Schooling Fish

Master thesis

by
Andrej Warkentin
Bernstein Center for Computational Neuroscience - Berlin

Supervisors:
Dr. Pawel Romanczuk
Bernstein Center for Computational Neuroscience - Berlin
Prof. Dr. Henning Sprekeler
Technische Universität Berlin

Contents

Abstract

Many aspects of fish school behavior can be explained qualitatively by self-propelled agent models with social interaction forces that are based on either metric or topological neighborhoods. Recently, startling of fish has been analyzed in its dependence of the network structure (Rosenthal et al., 2015) but a mechanistic model and its influence on the collective behavior is missing. Here we couple a model for collective behavior with a neuronal model that receives looming visual stimulus input to initiate a startle response, inspired by the neurobiologically well-studied Mauthner cell system. First, we analyzed the basic properties of the startle behavior of a single fish as a reaction to a looming stimulus. On the group level, we looked at startling frequency as well as group cohesion and polarization depending on neuronal and collective behavior parameters via simulations of the combined model. Our results indicate that the startling frequency strongly depends on the dynamics of the group structure, e.g. when the group approaches a boundary of the arena. In summary, we took first steps towards a biologically plausible model for startle response initiation in the context of collective motion.

1 Introduction

A common interpretation of the function of the nervous system in animals is to use the sensory input in order to make appropriate actions. One situation where this would be useful for the animal is the sudden appearance of a predator. The quick response to such a sudden, unexpected stimulus is called startle response and can be observed in many species (Eaton, 1984). In fish, the startle response can take the form of freezing, where the fish stops moving entirely, or the form of an escape response, where it quickly accelerates and moves away within less than a second. Escape responses in fish, also called fast starts, can be divided into the three stages 1) first body bend, 2) second body bend and a third, variable stage where the fish either goes into continuous swimming, coasting or braking (Domenici, 2011). Due to the body shape at the end of the first stage escape responses are also called C-start or S-start (Domenici, 2011)[1]. This thesis will focus on the C-start behavior of fish.
The C-start behavior in fish has been extensively studied and one of the main reasons for this is that a pair of neurons that play a major role in the initiation of the C-start, have large soma and axons and are therefore relatively easy to find in experiments. They are called Mauthner cells (M-cells), named after Ludwig Mauthner who first found and described their axons (Mauthner, 1859).
Before going into the details of the M-cell circuit we will give a brief overview of the nervous system of fish to provide some context. Since we will later focus on visually evoked C-starts we will go into more detail when it comes to the visual pathways in the brain. The overall structure of the nervous system of fish is very similar to mammals. Starting at the caudal end there is the spinal cord with descending motor pathways and the ascending sensory pathways. The spinal cord goes over into the hindbrain region with the medulla and the cerebellum. This is followed by the midbrain which comprises the rostral part of the brainstem and a roof region, the tectum **the chapter in encyclopedia of fish physiology** The remaining forebrain consists of the diencephalon and the telencephalon. In terms of sensory organs fish are equipped with the same senses as mammals and additionally have the lateral line organ that senses lower frequency signals around the body such as e.g. water flow and in some cases organs that can sense electrical fields.
Going from outside to inside, the eyes, again similar to mammals, consist of the cornea, the lens surrounded by the iris and the retina followed by the photoreceptors which build the most inside layer. In contrast to mammals the pupils of fish are not responsive to the amount of light in the environment. Fish mostly have rods and three different cones although across species there are up to seven different types of cones. The retina has different types of neurons that build different layers. The output neurons of the retina are the ganglion cells which show different kinds of tuning and whose axons build the optic nerve when they exit the eye. Although most fish don't have a fovea as we know it from humans there are retinal areas of higher ganglion cell and photoreceptor densities (Pita et al., 2015). Most of the ganglion cell axons cross sides and end up in the optic tectum which is the equivalent to the mammalian superior colliculus. While in humans much of the visual information goes further to the primary visual cortex in fish the optic tectum is the main site of processing of visual information. Similar to cortical areas it is comprised of different layers, also receiving input from other senses and other brain areas such as the telencephalon. The output of the optic tectum goes, among other regions, to the reticular nuclei in the hindbrain where we also find the Mauthner cell and can thus come the M-cell circuit.
The M-cell is located in the hindbrain and has two major dendritic branches, the ventral dendrite and the lateral dendrite. It receives multisensory input which is divided between the two dendritic branches. The lateral dendrite receives auditory and lateral line input whereas the ventral dendrite receives visual input via the optic tectum mentioned before. While this means that the visual input is highly processed by the networks in retina and optic tectum before it arrives at the M-cell the auditory input comes directly from the auditory nerve.

[1] It should be noted here that not all C-starts are escape responses because they can also be involved in e.g. prey capture but we will ignore other roles in the following.

This might be one of the reasons why the physiology of the auditory input has been studied in more detail than the visual part. We will therefore continue to describe the properties of the auditory processing and will have to assume that they also hold for the processing of the visual input. The synapses between auditory nerve and lateral dendrite are called club endings and transmit auditory signals via electrical as well as chemical mechanisms which leads to Excitatory Post-Synaptic Potentials (EPSPs) that consist of a fast and a slow component (Korn et al., 2005). At the same time the auditory nerve excites an interneuron which itself inhibits the M-cell. One interpretation of this feed-forward inhibition (FFI) is to increase the threshold for initiating the startle response. But this is not the only function of these interneurons because they also inhibit the contralateral M-cell as well as their contralateral counterparts (Koyama et al., 2016).
This microcircuit is probably responsible for the decision of which direction to escape to. To illustrate why this connectivity makes sense in this decision-making context, let us consider an auditory stimulus coming from the left side: It will inhibit the M-cell on the right side, inhibit the interneurons on the right side and excite the M-cell on the left side. Effectively, we have an increased inhibition of the right M-cell, decreased inhibition of the left M-cell and increased excitation of the left M-cell. Because the axons of the M-cells cross sides, an action potential of the M-cell on the left side will lead to a contraction of muscles on the right side, resulting in movements of head and tail away from the stimulus on the left side.
There are further properties that seem to make the M-cell specialized for initiating the C-start. Additional to the feed-forward inhibition the big size of the some of the M-cell leads to a high input resistance which again increases the threshold for incoming currents to initiate an action potential. The axon of the M-cell is unusually big as well which results in a fast signal transmission when an action potential is initiated and thus allows for fast reactions. The axon is also connected to interneurons that provide feedback inhibition to both M-cells. This is thought to prevent repetitive firing of the M-cell that fired in the first place and also to prevent the contralateral M-cell to fire shortly after. Apart from this feedback inhibition the axon goes through the whole spinal chord with colaterals that go to the motor neurons on the contralateral side. And also at this level we have again interneurons that putatively have the role of inhibiting a different set of motor neurons that are responsible for steady swimming movements (Song et al., 2015).
The exact role of the M-cells and the surrounding circuit in the C-start behavior is still a subject of study. The current state of research suggests that the M-cell is sufficient and necessary to evoke the first phase of short-latency C-starts. Nevertheless, if the M-cell is ablated the fish are still able to perform long-latency C-starts (Lacoste et al., 2015, Dunn et al., 2016). Furthermore, there is another population of neurons, that, if ablated, increase the latency of C-starts in a similar manner as the ablation of the M-cell does (Lacoste et al., 2015).
In the first part of this thesis we will make first steps towards a mechanistic understanding of functional role of the M-cell circuit for the C-start behavior. For this, we will greatly simplify the physiological properties of the M-cell and use a Leaky Integrate-and-Fire (LIF) model to capture the relevant dynamics. We did not choose the more realistic Hodgkin-Huxley like model type that takes into account different ion currents because we were not interested in the action potential shape but rather in the action potential timing dependent on the input. The simpler LIF model also allowed for more efficient simulation which was also useful for the integration of the neuronal model in the collective behavior model in the second part. For the input of the M-cell we will assume that the visual input, coming from the optic tectum, is the result of a feature extraction of the visual scene. Taken together, this will allow us to link parameters of the neuronal model to behavioral response properties and to compare and fit this to experimental data.
While the first part of the thesis is concerned with the behavior of single fish, for many fish species the natural environment is more likely to live in a group together with many other fish. Such groups of fish that move around together are called shoals if they are rather uncoordinated and schools if they move in a highly ordered manner. This collective behavior is not well understood yet and in the second part of this thesis we want to analyze how the startle response interacts with it. In more detail, we were interested in the following questions: Can the startle response be evoked spontaneously in the fish school e.g. when neighboring fish come too close too fast? Does the startling of a single fish spread in the school? How do these effects depend on the properties of the school?

In order to address these questions we will use an agent-based model that describes the interactions between fish by so-called social forces. Typically, there are the three forces repulsion, alignment and attraction and they can work either on neighbors within a specific range (metric interaction) or only on topological neighbors (topological interaction). An example for a topological type of interaction would be to only consider the neighboring cells of the Voronoi tessellation of the group of fish. Using such an agent-based collective behavior model with metric interaction, Couzin et al., 2002 could show that the simulated fish school shows different modes of behavior dependent on the parameters of the social forces. While in one mode the collective would be uncoordinated but stay loosely together, it would move highly polarized and cohesive in another parameter regime or show a kind of milling behavior in a third mode.

2 Single Mauthner Cell Model - Theory

In this chapter we will explain the theoretical aspects of the neuronal model for a single Mauthner Cell. By 'single' Mauthner cell we only mean that we are considering the mechanisms of the surrounding circuit involving one of the two existing Mauthner cells instead of both. We will start with the description of the full model and continue with two reductions that assume a separation of timescales and thus provide stationary approximations of the model.

2.1 Full neuronal model

The full neuronal model of a single Mauthner cell consists of a rate-based model for the population of inhibitory interneurons that provide the feed-forward inhibition and a LIF model for the M-cell itself. Both the inhibitory population and the M-cell get their input from a single source. In our case this input will represent the visual information coming from the optic tectum which will be described in more detail in the next chapter. The time evolution of the activity ρ of the inhibitory population is described by the following equation:

$$\tau_\rho \frac{d\rho}{dt} = -(\rho(t) - \rho_0) + c_\rho I(t) + \eta_\rho, \tag{2.1}$$

where τ_ρ is the time constant, ρ_0 is the resting activity of the population, c_ρ is a scaling factor, $I(t)$ is the time dependent input and η_ρ is a Gaussian noise term. For the M-cell we use a LIF model where the time evolution of the membrane potential V_m is described by the following equation:

$$\tau_m \frac{dV_m}{dt} = -(V(t) - E_L) + R_m I(t) - \rho(t) + \eta_m, \tag{2.2}$$

where τ_m is the membrane time constant, E_L is the resting potential, R_m is the membrane resistance and η_m is again a Gaussian noise term. The M-cell thus gets the direct visual input $I(t)$ and is inhibited by $\rho(t)$. If the membrane potential V_m crosses a threshold V_t an action potential is artificially produced and the membrane potential is reset to the resting potential E_L. Additional to the noise terms in equations 2.1 and 2.2 we will also consider fluctuations of the firing threshold V_t:

$$V_t(t) = V_t + \eta_t, \tag{2.3}$$

where η_t is a Gaussian noise term.
The basic parameters of the LIF model, i.e. E_L, R_m, τ_m and V_t, have been fitted to experimental data in a previous study by Koyama et al., 2016 using recordings from four zebrafish at four days post-fertilization(dpf). For the details of the fitting procedure see their methods section.
One important property of this dynamic system are the time scales on which the described activity is going on. Since we know that the synapses at the inhibitory interneurons are electric, at least for the auditory input, the time constant, and therefore the relevant time scale, of ρ is in the order of milliseconds. As we will see later on, in the experiments that we want to reproduce the changes in the input over time are on much bigger time scales of at least hundreds of milliseconds. This fact motivates the reduction in the next section where we approximate the activity of the inhibitory population by the stationary solution.

2.2 Stationary Approximation of Inhibitory Population

Here we reduce the model by approximating the activity of the inhibitory population by its stationary solution. This approximation is the more accurate the higher the difference is between the time scale of the dynamics of the inhibitory population and the time scale of

the input. If we use τ_ρ as the time scale of the inhibitory population and denote τ_{in} as the time scale of the input, the approximation becomes equivalent for the limit $\tau_\rho/\tau_{in} \to 0$. In the model, this means that equation 2.1 becomes:

$$\hat{\rho}(t) = \rho_0 + c_\rho I(t) + \eta_\rho. \tag{2.4}$$

Now we can replace $\rho(t)$ in equation 2.2 and get:

$$\tau_m \frac{dV_m}{dt} = -(V(t) - E_L) + I(t)(R_m - c_\rho) - \rho_0 - \eta_\rho + \eta_m. \tag{2.5}$$

In the resulting LIF model the input is now weighted by the difference between the scaling factor c_ρ and the membrane resistance R_m. If we ignore the noise terms for a moment and assume that $\rho_0 = 0$, this means that the input can only excite the M-cell and therefore evoke an action potential if $c_\rho < R_m$. Increasing ρ_0 would effectively increase the firing threshold V_t.

2.3 Stationary Approximation of Full Model

As a next step we can further approximate the LIF model in equation 2.5 by its stationary solution:

$$\hat{V}_m(t) = E_L + I(t)(R_m - c_\rho) - \rho_0 - \eta_\rho + \eta_m. \tag{2.6}$$

If we set all noise to zero we can derive an expression for the input at which the membrane potential reaches the threshold V_t:

$$\hat{V}_m(t) \stackrel{!}{=} V_t \tag{2.7}$$

$$\Leftrightarrow E_L + I(t)(R_m - c_\rho) - \rho_0 \stackrel{!}{=} V_t \tag{2.8}$$

$$\Leftrightarrow I(t) \stackrel{!}{=} \frac{V_t - E_L + \rho_0}{(R_m - c_\rho)} \tag{2.9}$$

- maybe discuss relation to first-passage time problems

3 Single Mauthner Cell Model - Numerical experiments

We will now come to the simulations of the visual looming stimulus experiment. For this we first describe the experiments that we want to reproduce, especially the specific conditions and results. This is followed by the results of the simulations using the model in the different formulations that we showed in the previous chapter. Furthermore, we fit the parameters of the full model to experimental data and finally summarize and discuss our findings.

3.1 Visual looming stimulus experiments

One of the earliest visual looming stimulus experiments has been conducted by Dill, 1974 where they photographed a black dot on a white background and projected these photographs on a tracing paper that was taped to the wall of the aquarium and thus creating a virtual looming stimulus. They also tested a model predator that consisted of a black disk of Plexiglas that was moved by a motor. In more recent studies computer-generated stimuli are used and therefore the stimulus size and velocity can be controlled more precisely.
The typical arrangement is a small dish or aquarium in which a single fish can either freely move or it is head-restrained, i.e. it can only move its tail while the head is fixed. In the studies that we will consider here they used larval zebrafish (Temizer et al., 2015, Dunn et al., 2016, Bhattacharyya et al., 2017) and in one case they used goldfish (Preuss et al., 2006). The stimulus is then either projected on the floor, ceiling or side wall of the aquarium or a screen is placed close to the aquarium. In most studies the stimulus is a black disk or square on a white or blue background. Other stimuli that have been tested, such as a circle with a checkerboard pattern did not show significant differences (Preuss et al., 2006, Dunn et al., 2016) but there has been no systematic analysis . The stimulus sizes, i.e. the diameter of the disk or the side length of the square, range from 0.3 mm to 5 cm and the velocities range from 0.2 cm/s to 60 cm/s. Another parameter that is often reported is the ratio of stimulus size and velocity, L/V, which indicates the time needed to cover a distance of a length equal to the stimulus size. The subtended visual angles on the retina of the fish range from 2°to at least 100°. For an overview of all reported conditions in the experiments see Table 3.1.
For the results of the experiment the time from onset of the stimulus (latency), the distance and the visual angle are measured at the time when the fish responds, i.e. starts to move away. The visual angle at response time (response angle) has been found to have the same mean value at different stimulus sizes and velocities in all studies that were done with zebrafish, although there are substantial differences in the mean value as well as in the variance. This could be explained by the differences in various experimental conditions such as the water temperature, head restraining or the acclimation time (see Table 3.1). While the study with goldfish (Preuss et al., 2006) does not report to find a so-called critical visual angle, the observed response angles (14°to 29°) are in a range that is comparable to e.g. the one found by Bhattacharyya et al., 2017 (35°± 15°).
For the simulations of the experiment we closely followed the procedure reported by Bhattacharyya et al., 2017. At the beginning of a trial a stimulus size is drawn from a uniform distribution between 10 mm and 25 mm. Next, an L/V value is uniformly drawn between 0.1 s and 1.2 s and the resulting velocity for the trial stimulus size is calculated. With the trial stimulus size L_{trial} and the trial velocity v_{trial} the visual angle over time $\theta(t)$ is calculated by:

$$\theta(t) = 2 \cdot \arctan(\frac{L_{trial}/2}{D_{init} - v_{trial} \cdot t}), \tag{3.1}$$

where D_{init} is the virtual initial distance which is set to 50mm if not stated otherwise. The range of possible time courses of the visual angle is shown in Figure 3.1 A. Note that because the initial distance is fixed and we sample from different stimulus sizes we get different initial angles for the same L/V values. This leads to different time courses for the same L/V value

Study	**1**	**2**	**3**	**4**
Species	Zebrafish	Zebrafish	Zebrafish	Goldfish
Age	6-8 dpf	5-6 dpf	5 - 7 dpf	-
Water temperature [°C]	28	-	24	18
Screen spanning angle horizontal [°]	62	>100*	>70*	-
Screen spanning angle vertical [°]	50	-	-	-
Screen distance [cm]	1	-	3.25	16
Luminance dark	0.07 cd/m^2	0.7 lux	-	70-80 lux
Luminance grey	-	75 lux	-	-
Luminance white	122.5 cd/m^2	512 lux	500 lumen	300-320 lux
L/V values [ms]	60-300 †	510 - 2900 †	100 - 1200	20 - 110*
Durations [s]	1.65 - 8	0.5 - 5*	1 - 5.5*	0.25 - 0.8*
Acclimation time [min]	-	-	15	-
Visual angles [°]	2 - 48	25 - 100*	8 - 70*	2 - 100*
Critical angle [°]	21.7 ± 2.5	72 ± 1.3	35 ± 15	-
Response probabilities	20 - 75*	46 - 60	25 - 75*	70 - 91
Head-restrained	Yes	No	No	No
Stimulus shape	Circle	Circle	Rectangle	Circle
Stimulus color	Black/White,	Black/Chkb.	Black	Black
Background color	White/Black,	Grey	Blue	White
Stimulus sizes [cm]	0.03	?	1 - 2.5	0.5 - 5*
Stimulus velocities [cm/s]	0.2 - 1	?	?	20 - 60
Initial distances (virtual) [cm]	?	?	5	?
Projection site	Side/Front	Bottom	Side/Front	Above

Table 3.1 – The corresponding references of the studies are 1: Temizer et al., 2015, 2: Dunn et al., 2016, 3: Bhattacharyya et al., 2017 and 4: Preuss et al., 2006. Note that the studies might have conducted other looming stimulus experiments with simultaneous neural recordings but they are not included here because this project is restricted to the behavioral aspects. For values denoted with a "†" we used the diameter instead of the radius, as it was done in the original studies. Values with an "*" are either read of figures or inferred from other, reported values. Chkb. = Checkerboard pattern.

depending on the stimulus size but starting from the same angle their time courses are identical (Figure 3.1 B). If we now assume a critical angle θ_{crt} at which the fish escapes, we can describe how the response time, response distance and time-to-collision (TTC) at response depend on the L/V value. The response time linearly depends on the L/V while the slope of the relationship is determined by stimulus size L, initial distance D_{init} and critical angle θ_{crt}:

$$t_{resp} = \frac{L}{v}\left(\frac{D_{init}}{L} - \frac{1}{2 \cdot \tan(\theta_{crt}/2)}\right). \tag{3.2}$$

The response distance only depends on the stimulus size L:

$$D_{resp} = \frac{L}{2 \cdot \tan(\theta_{crt}/2)}. \tag{3.3}$$

The TTC linearly depends on L/V and the slope is determined only by the critical angle θ_{crt}:

$$TTC_{resp} = -\frac{L}{2 \cdot v \cdot \tan(\theta_{crt}/2)}. \tag{3.4}$$

For an example with $\theta_{crt} = 35$ and $D_{init} = 50$ these idealized response properties are illustrated in Figure 3.2, where we chose the same axes as in Figure 1 of Bhattacharyya et al., 2017 for easy comparison.
In our simulations the visual angle is next transformed by a linear function and the result is the input $I(t)$ for our neuronal model, described in the previous chapter:

$$I(t) = f(\theta(t)) = m \cdot \theta(t) + b. \tag{3.5}$$

In order to calculate the response properties we take the time of the first spike t_{spk} of the model M-cell after stimulus onset as the response time of the fish. We ignore further processing time after the spike because it is in the order of milliseconds (Preuss et al., 2003) and thus irrelevant with respect to the overall response time which is in the order of at least hundreds of milliseconds for visual stimuli (Preuss et al., 2006). Thus the response angle of the simulated trial will be $\theta(t_{spk})$.

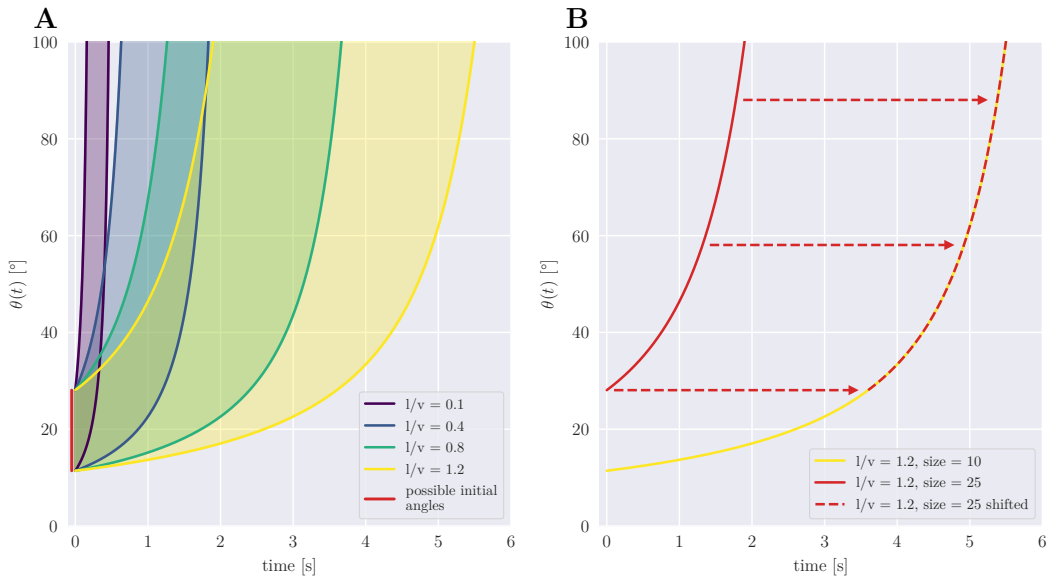

Figure 3.1 – Range of time courses of θ depending on L/V. **A** For four different L/V values the possible time courses are shown if stimulus size L ranges between 10 mm and 25 mm. **B** Single time courses for the same L/V value only differ in a horizontal shift that is introduced by the different initial angle.

3.2 Stationary model prediction

$$I(t) = 10^{-11} c_{exc} f(\theta(t)) = 10^{-11} c_{exc}(m \cdot \theta(t) + b) \tag{3.6}$$

Inserting values for the fixed parameters $E_L = -79$ mV, $R_m = 10$ MΩ and $V_t = -61$ mV:

$$-0.079 + 10^7 I(t) - c_\rho 10^7 I(t) - \rho_0 \overset{!}{=} -0.061 \tag{3.7}$$

$$\Leftrightarrow 10^7 I(t) - c_\rho 10^7 I(t) - \rho_0 \overset{!}{=} 0.018 \tag{3.8}$$

$$\Leftrightarrow 10^{-4} c_{exc} f(\theta(t))(1 - c_\rho) - \rho_0 \overset{!}{=} 0.018 \tag{3.9}$$

$$\Leftrightarrow f(\theta(t)) \overset{!}{=} \frac{180 + \rho_0 10^4}{c_{exc}(1 - c_\rho)} \tag{3.10}$$

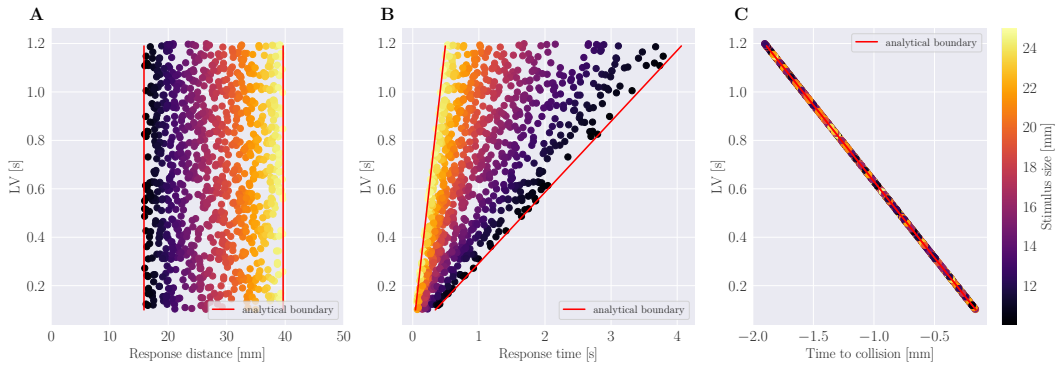

Figure 3.2 – Response properties for a critical angle $\theta_{crt} = 35$ and initial distance $D_{init} = 50mm$. For all plots L was sampled between 10 mm and 25 mm and L/V was sampled between 0.1 s and 1.2 s. Red lines show minimal and maximal values calculated using Equations 3.2, 3.3 and 3.4. **A** The response distance only depends on L and thus has the same range for all L/V values. **B** Response times linearly increase with L/V and the slope increases for smaller L. **C** Absolute time-to-collision linearly increases with L/V and the slope only depends on θ_{crt}.

$$\Leftrightarrow \theta(t) \stackrel{!}{=} \frac{180 + \rho_0 10^4}{m \cdot c_{exc}(1 - c_\rho)} - \frac{b}{m} \tag{3.11}$$

3.3 Chapter outline

- results for the minimal model aka the noiseless, stationary solution:
  - we know expression for critical input from equation 2.9
  - if we insert our expression for the visual looming stimulus we get this critical angle as a function of the free parameters: show equation
  - optional: what happens if we use sigmoid function instead of linear?
- results for simple LIF model where inhibitory population activity is approximated:
  - show response properties (only 2 or 3 as the others are redundant) and their dependence on free parameters:
  - also always include stationary solution from previous section for comparison
  - also show preuss data
- results for full model:
  - show effect of additional parameter τ_ρ
- fitting of parameters:
  - we will only use raw data that we got from Bhattacharyya et al., 2017 bc it's from zebrafish where we have the fitted parameters from Koyama et al., 2016
  - give brief summary of fitting procedure from Lueckmann et al., 2017
  - describe chosen meta parameters for fitting: layers, neurons per layer, nepochs, ntraining runs etc.
  - show fitting results
- discussion of results:
  - summarize results
  - mention stimulus time scales
  - unifying theory that combines bhattacharyya data and preuss data?!
  - do fitted parameters make sense?

Parameter	**Value (unit)**	**Comment**
E_L	-79 mV	Resting potential
R_M	10 MOhm	Membrane resistance
τ_m	23 ms	Membrane time constant
V_t	-61 mV	Mean spiking threshold
dt	0.001 s	Integration time step
T	5 s	Total time
sd_{thr}	1 mV	Standard deviation of spiking threshold noise
sd_I	5 mV	Standard deviation of input noise
sd_{init}	1 mV	Standard deviation of initial condition noise
m	1 °/s	Slope of linear transformation
b	0 °	Offset of linear transformation

Table 3.2 – Parameters of the single LIF neuron model with a looming stimulus input. Parameters that were explored are indicated either by a value range such as e.g. for μ_s or by a set with all explored values inside of curly brackets such as e.g. for σ_s.

4 Coupling of Neuronal Model and Collective Dynamics

- description behavioral experiments:
  - schooling behavior in general has been analyzed
  - startling in schools has not been studied so much (except maybe Fischer et al., 2015)
  - but there is study by Rosenthal et al., 2015
  - summarize experiment and findings
- description schooling model:
  - movement equations, social forces (take from lab report)
  - describe coupling: every agent integrates visual info (how will be described in next section)
  - decision: on what level should we implement the variability of rho null? over time or across fish? we chose across fish here, assuming they are in different internal states, maybe also with different characters (cite paper about dominance Khan et al., 2017, Miller et al., 2017, Neumeister et al., 2010, Park et al., 2018)
- how to integrate visual info/couple input from different neighbors
  - mention ensemble statistics (see paper that pawel sent me)
  - what we will look at: global mean/max/deviate, knn mean/deviate
- simulation results:
  - show startle frequency, density and polarization for the different integration strategies
  - show effect of school position on startle probability
  - show cascade sizes as function 1)input scaling 2) school structure, order, density

5 Discussion

- we focus here on the experimental results from Bhattacharyya et al., 2017 but one should keep in mind that their results might be specific to properties of experiment such as fish handling, fish age, species, arena, environment, stimulus setup (projection on screen)
- we took the fitted parameters from Koyama et al., 2016 but those are fitted for their specific context which might vary in other experimental conditions and certainly in other species
- furthermore the LIF model makes strong assumptions about the processing power of the neuron which are likely not true. see for example Koch et al., 2000, and specifically for M-cell Medan et al., 2017
- in locusts, neurons have been found that specifically code looming stimuli Hatsopoulos et al., 1995 (?)
- we should keep in mind that the optic tectum is still developing at larval stage Avitan et al., 2017
- considering the amount of differences of previous studies that looked into visual looming stimuli, a more systematic analysis of visually evoked startle responses in zebrafish is clearly missing
- test citations: Severi et al., 2014, Sarvestani et al., 2013, Romano et al., 2015, Parrish et al., 2002, Møller, 1989, Howe et al., 2013, Del Bene et al., 2010

Bibliography

Avitan, Lilach et al. (2017). "Spontaneous Activity in the Zebrafish Tectum Reorganizes over Development and Is Influenced by Visual Experience". In: Current Biology 27.16, 2407–2419.e4. ISSN: 0960-9822. DOI: 10.1016/j.cub.2017.06.056. URL: http://www.sciencedirect.com/science/article/pii/S0960982217307935.

Bhattacharyya, Kiran, David L. McLean, and Malcolm A. MacIver (2017). "Visual Threat Assessment and Reticulospinal Encoding of Calibrated Responses in Larval Zebrafish". In: Current Biology 27.18, 2751–2762.e6. ISSN: 0960-9822. DOI: 10.1016/j.cub.2017.08.012. URL: http://www.sciencedirect.com/science/article/pii/S0960982217310217.

Couzin, Iain D., Jens Krause, Richard James, Graeme D. Ruxton, and Nigel R. Franks (2002). "Collective Memory and Spatial Sorting in Animal Groups". In: Journal of Theoretical Biology 218.1, pp. 1–11. ISSN: 0022-5193. DOI: http://dx.doi.org/10.1006/jtbi.2002.3065. URL: http://www.sciencedirect.com/science/article/pii/S0022519302930651.

Del Bene, Filippo et al. (2010). "Filtering of Visual Information in the Tectum by an Identified Neural Circuit". In: Science 330.6004, pp. 669–673. ISSN: 0036-8075. DOI: 10.1126/science.1192949. eprint: http://science.sciencemag.org/content/330/6004/669.full.pdf. URL: http://science.sciencemag.org/content/330/6004/669.

Dill, Lawrence M. (1974). "The escape response of the zebra danio (Brachydanio rerio) I. The stimulus for escape". In: Animal Behaviour 22.3, pp. 711–722. ISSN: 0003-3472. DOI: https://doi.org/10.1016/S0003-3472(74)80022-9. URL: http://www.sciencedirect.com/science/article/pii/S0003347274800229.

Domenici, P. (2011). "BUOYANCY, LOCOMOTION, AND MOVEMENT IN FISHES | Fast Start". In: Encyclopedia of Fish Physiology. Ed. by Anthony P. Farrell. San Diego: Academic Press, pp. 587–596. ISBN: 978-0-08-092323-9. DOI: 10.1016/B978-0-12-374553-8.00215-X. URL: https://www.sciencedirect.com/science/article/pii/B978012374553800215X.

Dunn, Timothy W. et al. (2016). "Neural Circuits Underlying Visually Evoked Escapes in Larval Zebrafish". In: Neuron 89.3, pp. 613–628. ISSN: 0896-6273. DOI: 10.1016/j.neuron.2015.12.021. URL: http://www.sciencedirect.com/science/article/pii/S089662731501123X.

Eaton, R.C. (1984). Neural Mechanisms of Startle Behavior. Springer. ISBN: 9780306415562. URL: https://books.google.de/books?id=eNdUpgSOWMoC.

Fischer, Eva K., Adina J. Schwartz, Kim L. Hoke, and Daphne Soares (2015). "Social Context Modulates Predator Evasion Strategy In Guppies". In: Ethology 121.4. ETH-14-0189, pp. 364–371. ISSN: 1439-0310. DOI: 10.1111/eth.12345. URL: http://dx.doi.org/10.1111/eth.12345.

Hatsopoulos, Nicholas, Fabrizio Gabbiani, and Gilles Laurent (1995). "Elementary Computation of Object Approach by a Wide-Field Visual Neuron". In: Science 270.5238, pp. 1000–1003. ISSN: 0036-8075. DOI: 10.1126/science.270.5238.1000. eprint: http://science.sciencemag.org/content/270/5238/1000.full.pdf. URL: http://science.sciencemag.org/content/270/5238/1000.

Howe, Kerstin et al. (2013). "The zebrafish reference genome sequence and its relationship to the human genome." In: Nature 496 (7446), pp. 498–503. ISSN: 1476-4687. DOI: 10.1038/nature12111.

Khan, Kanza M. and David J. Echevarria (2017). "Feeling Fishy: Trait Differences in Zebrafish (Danio Rerio)". In: Personality in Nonhuman Animals. Springer International Publishing, pp. 111–127. DOI: 10.1007/978-3-319-59300-5_6.

Koch, Christof and Idan Segev (2000). "The role of single neurons in information processing". In: NATURE NEUROSCIENCE 3.11, S, 1171–1177. ISSN: 1097-6256. DOI: {10.1038/81444}.

Korn, Henri and Donald S Faber (2005). "The Mauthner cell half a century later: a neurobiological model for decision-making?" In: Neuron 47 (1), pp. 13–28. ISSN: 0896-6273. DOI: 10.1016/j.neuron.2005.05.019.

Koyama, Minoru et al. (2016). "A circuit motif in the zebrafish hindbrain for a two alternative behavioral choice to turn left or right". In: ELIFE 5. ISSN: 2050-084X. DOI: 10.7554/elife.16808.

Lacoste, Alix M. B. et al. (2015). "A Convergent and Essential Interneuron Pathway for Mauthner-Cell-Mediated Escapes". In: CURRENT BIOLOGY 25.11, 1526–1534. ISSN: 0960-9822. DOI: 10.1016/j.cub.2015.04.025.

Lueckmann, Jan-Matthis et al. (2017). "Flexible statistical inference for mechanistic models of neural dynamics". In: Advances in Neural Information Processing Systems 30. Ed. by I. Guyon et al. Vol. 38. Curran Associates, Inc., pp. 1289–1299. URL: http://papers.nips.cc/paper/6728-flexible-statistical-inference-for-mechanistic-models-of-neural-dynamics.pdf (visited on 03/26/2018).

Mauthner, Ludwig (1859). "Untersuchungen uber den Bau des Ruckenmarkes der Fische: Eine vorlaufige Mittheilung". In: Sitzungsberichte der Kaiserlichen Akademie der Wissenschaften. Mathematisch 34, pp. 31–36.

Medan, Violeta, Tuomo Mäki-Marttunen, Julieta Sztarker, and Thomas Preuss (2017). "Differential processing in modality-specific Mauthner cell dendrites". In: The Journal of Physiology, n/a–n/a. ISSN: 1469-7793. DOI: 10.1113/JP274861. URL: http://dx.doi.org/10.1113/JP274861.

Miller, Thomas H. et al. (2017). "Social Status–Dependent Shift in Neural Circuit Activation Affects Decision Making". In: Journal of Neuroscience 37.8, pp. 2137–2148. ISSN: 0270-6474. DOI: 10.1523/JNEUROSCI.1548-16.2017. eprint: http://www.jneurosci.org/content/37/8/2137.full.pdf. URL: http://www.jneurosci.org/content/37/8/2137.

Møller, J. (1989). "Random tessellations in $\mathbb{R}^d$". In: Advances in Applied Probability 21.1, pp. 37–73. DOI: 10.1017/S0001867800017195.

Neumeister, H., K. W. Whitaker, H. A. Hofmann, and T. Preuss (2010). "Social and Ecological Regulation of a Decision-Making Circuit". In: JOURNAL OF NEUROPHYSIOLOGY 104.6, 3180–3188. ISSN: 0022-3077. DOI: 10.1152/jn.00574.2010.

Park, Choongseok, Katie N. Clements, Fadi A. Issa, and Sungwoo Ahn (2018). "Effects of Social Experience on the Habituation Rate of Zebrafish Startle Escape Response: Empirical and Computational Analyses". In: Frontiers in Neural Circuits 12, p. 7. ISSN: 1662-5110. DOI: 10.3389/fncir.2018.00007. URL: https://www.frontiersin.org/article/10.3389/fncir.2018.00007.

Parrish, Julia K., Steven V. Viscido, and Daniel Grünbaum (2002). "Self-Organized Fish Schools: An Examination of Emergent Properties". In: The Biological Bulletin 202.3. PMID: 12087003, pp. 296–305. DOI: 10.2307/1543482. eprint: https://doi.org/10.2307/1543482. URL: https://doi.org/10.2307/1543482.

Pita, Diana, Bret A. Moore, Luke P. Tyrrell, and Esteban Fernández-Juricic (2015). "Vision in two cyprinid fish: implications for collective behavior". In: PeerJ 3, e1113. ISSN: 2167-8359. DOI: 10.7717/peerj.1113. URL: https://doi.org/10.7717/peerj.1113.

Preuss, Thomas and Donald S. Faber (2003). "Central Cellular Mechanisms Underlying Temperature-Dependent Changes in the Goldfish Startle-Escape Behavior". In: Journal of Neuroscience 23.13, pp. 5617–5626. ISSN: 0270-6474. eprint: http://www.jneurosci.org/content/23/13/5617.full.pdf. URL: http://www.jneurosci.org/content/23/13/5617.

Preuss, Thomas, Princess E. Osei-Bonsu, Shennan A. Weiss, C. Wang, and Donald S. Faber (2006). "Neural Representation of Object Approach in a Decision-Making Motor Circuit". In: Journal of Neuroscience 26.13, pp. 3454–3464. ISSN: 0270-6474. DOI: 10.1523/JNEUROSCI.5259-05.2006. eprint: http://www.jneurosci.org/content/26/13/3454.full.pdf. URL: http://www.jneurosci.org/content/26/13/3454.

Romano, Sebastián A. et al. (2015). "Spontaneous Neuronal Network Dynamics Reveal Circuit's Functional Adaptations for Behavior". In: Neuron 85.5, pp. 1070–1085. ISSN: 0896-6273. DOI: https://doi.org/10.1016/j.neuron.2015.01.027. URL: http://www.sciencedirect.com/science/article/pii/S0896627315000537.

Rosenthal, Sara Brin, Colin R Twomey, Andrew T Hartnett, Hai Shan Wu, and Iain D Couzin (2015). "Revealing the hidden networks of interaction in mobile animal groups allows prediction of complex behavioral contagion." In: Proceedings of the National Academy of Sciences of the United 112 (15), pp. 4690–4695. ISSN: 1091-6490. DOI: 10.1073/pnas.1420068112.

Sarvestani, Iman Kamali, Alexander Kozlov, Nalin Harischandra, Sten Grillner, and Örjan Ekeberg (2013). "A computational model of visually guided locomotion in lamprey". In: Biological Cybernetics 107.5, pp. 497–512. ISSN: 1432-0770. DOI: 10.1007/s00422-012-0524-4. URL: https://doi.org/10.1007/s00422-012-0524-4.

Severi, Kristen E. et al. (2014). "Neural Control and Modulation of Swimming Speed in the Larval Zebrafish". In: Neuron 83.3, pp. 692–707. ISSN: 0896-6273. DOI: https://doi.org/10.1016/j.neuron.2014.06.032. URL: http://www.sciencedirect.com/science/article/pii/S0896627314005789.

Song, Jianren, Konstantinos Ampatzis, Jessica Ausborn, and Abdeljabbar El Manira (2015). "A Hardwired Circuit Supplemented with Endocannabinoids Encodes Behavioral Choice in Zebrafish". In: Current Biology 25.20, pp. 2610–2620. ISSN: 0960-9822. DOI: 10.1016/j.cub.2015.08.042. URL: http://www.sciencedirect.com/science/article/pii/S0960982215010131.

Temizer, Incinur, Joseph C. Donovan, Herwig Baier, and Julia L. Semmelhack (2015). "A Visual Pathway for Looming-Evoked Escape in Larval Zebrafish". In: Current Biology 25.14, pp. 1823–1834. ISSN: 0960-9822. DOI: 10.1016/j.cub.2015.06.002. URL: http://www.sciencedirect.com/science/article/pii/S0960982215006673.

.1 Appendix